Journal of Materials Chemistry C

Accepted Manuscript

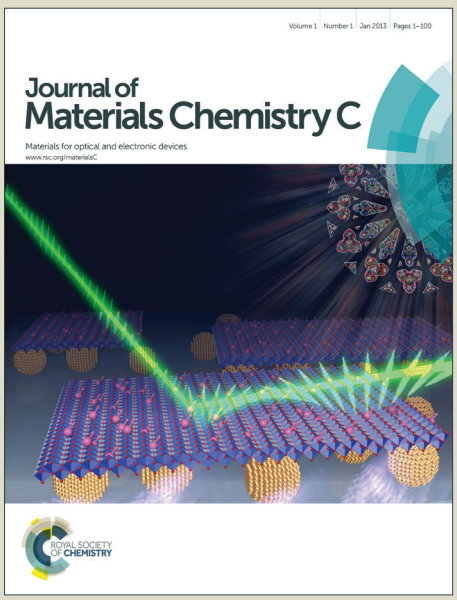

ROYAL SOCIETY OF CHEMISTRY

www.rsc.org/materialsC

Cite this: DOI: 10.1039/c0xx00000x

www.rsc.org/xxxxxx

ARTICLE TYPE

Thermal evaporation synthesis of SiC/SiO_x nanochain heterojunctions and their photoluminescence properties

Haitao Liu,[a] Zhaohui Huang,*[a] Juntong Huang,[ab] Minghao Fang,[a] Yan-gai Liu[a] and Xiaowen Wu[a]

Received (in XXX, XXX) Xth XXXXXXXXX 20XX, Accepted Xth XXXXXXXXX 20XX

DOI: 10.1039/b000000x

Core-shell SiC/SiO_x nanochain heterojunctions have been successfully synthesized on silicon substrate via a simplified thermal evaporation method at 1500 °C without using catalyst, template and flowing gases (Ar, CH_4, N_2, *etc.*). X-ray diffraction (XRD), field emission scanning electron microscopy (FESEM), transmission electron microscopy (TEM/HRTEM) equipped with energy-dispersive X-ray spectroscopy (EDS), scanning transmission electron microscopy (STEM) and Fourier-transform infrared spectroscopy (FT-IR) are used to characterize the phase composition, morphology, and microstructure of the as-received nanostructures. A combined vapor-solid (VS) growth and modulation procedure is proposed for the growth mode of the as-grown SiC/SiO_x nanochains. The formation of SiO_x beads not only relates to the Rayleigh instability and the poor wettability between SiC and SiO_x, but also corresponds to the existence of high stacking faults within SiC-core nanowires. The photoluminescence spectrum of the nanochains exhibits a significant blue-shift, which can be highly valuable for the future potential applications in blue-green emitting devices.

Introduction

One-dimensional (1-D) nanostructures, such as nanowires, nanobelts, nanotubes, nanocables and nanochains have become the focus of exhaustive research owing to their outstanding properties. [1-6] Among several unconventional 1-D nanostructures, 1-D heterostructures are appealing as a result of their potential applications in future nanodevices and nanoscale systems. [7-9] Up to present, tremendous efforts have been devoted to the growth of 1-D heterostructures, such as Si/Ge nanowire heterostructures, [10] ZnS/SiO_2 nanocables, [11] and Si/SiO_2 nanochains. [12] Among them, SiC 1-D heterojunctions, such as SiC/ZnO nanobrush heterojunctions, [13] SiC/BN nanocable heterojunctions, [14-15] SiC/Al_2O_3, [8] SiC/SiO_2, [9] SiC/SiO_2/C, [16] and SiC/C [17] nanowire heterojunctions have stimulated considerable interest due to their excellent properties (*i.e.* high mechanical strength, high thermal conductivity, high chemical stability, and high thermal stability, *etc.*).

Nanochain is one of the most important 1-D heterojunctions with excellent properties. SiC/SiO_2 nanochain heterojunction has attracted much attention since it can couple with the unique properties of SiC and SiO_x. [18, 19] Up to now, several preparation methods have been used to synthesize the SiC/SiO_2 nanochain heterojunction. Li *et al.* [6] prepared SiC/SiO_2 chainlike nanostructures via a template/catalyst-free chemical vapor reaction process using Si-SiO_2 mixture powder and CH_4 as raw materials at 1200-1250 °C. Wei *et al.* [20] obtained 1-D SiC/SiO_2 nanochain heterojunctions via a microwave method using tetraethoxysilane (TEOS), Si and charcoal as raw materials. Hou *et al.* [21] reported the mass production of SiC/SiO_x nanochain heterojunctions via pyrolysis of polymeric precursors. Meng *et al.* [5] synthesized β-SiC nanochains by anodic aluminum oxide (AAO) template assisted chemical vapor reaction process. Just recently, Bechelany *et al.* [22] reported a two-step route to the synthesis of SiC/SiO_2 nanochains, and disclosed that the nanochains formation mechanism was attributed mainly to the Rayleigh instability. However, most of these reported methods involve complex equipments and processes.

On the basis of efficiency and economy, the carbothermal reduction process is considered to be a potential method for the synthesis of SiC nanostructures on account of its inexpensiveness and simplicity. In the present work, we report a simplified thermal evaporation method to prepare SiC/SiO_x nanochains without using catalyst, template and flowing gases (Ar, CH_4, N_2, *etc.*). It is promising that the present work could provide a novel and facile method for the growth of SiC/SiO_x nanochains.

Experimental

Core-shell SiC/SiO_x nanochain heterojunctions were grown directly on silicon substrate by a simplified thermal evaporation method without using catalyst, template and flowing gases (Ar, CH_4, N_2, *etc.*). A n-type Si (100) wafer (4 Ω•cm, Beijing Zhongkekenuo new energy technology Co. Ltd, China) of size 2 cm × 3 cm was used as the substrate. The surface of the silicon substrate was ultrasonically cleaned by acetone and ethanol for 10 minutes respectively, and then dried in air. The silicon wafer was placed in a small corundum crucible and covered by a cleaned graphite felt. After that, the cleaned system was

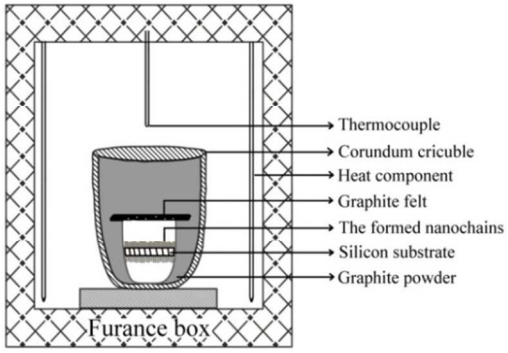

Scheme 1 Schematic experiment setup for SiC/SiO_x nanochain heterojunctions synthesis.

immerged in graphite powders inside a big enclosed corundum crucible. It is worth noting that several little holes on the cleaned graphite felt were stabbed by a needle to keep the atmospheric pressure balance between the big enclosed corundum and the small corundum. The aforementioned big enclosed corundum was then located in the crucible as shown in Scheme 1. The prepared system was heated in air atmosphere in a programmed way, from room temperature to 1000 °C at 10 °C/min, from 1000 °C to 1500 °C at 3 °C/min and maintained there for 3 h. After cooling to room temperature, a green colored layer was formed on the surface of the silicon wafer.

The as-prepared products were characterized by X-ray diffraction (XRD), field emission scanning electron microscopy (FESEM, JEOL JSM6700F, Japan), transmission electron microscopy (TEM/HRTEM, FEI-Tecnai-G^2-F20, Philips, Netherlands) equipped with energy-dispersive X-ray spectroscopy (EDS) and scanning transmission electron microscopy (STEM, FEI-Tecnai-G^2-F20, Philips, Netherlands). Fourier-transform infrared spectroscopy (FT-IR) data were collected on a Nicolet IR100/200 spectrophotometer over the wavenumbers range of 450-1500 cm^{-1}, and the standard KBr pellet technique was employed, in which the KBr pellets have been dried effectively. The room temperature photoluminescence (PL) property measurement was performed by a fluorescence spectrophotometer (Hitach F-4600, Japan) at room temperature from a Xe lamp excitation.

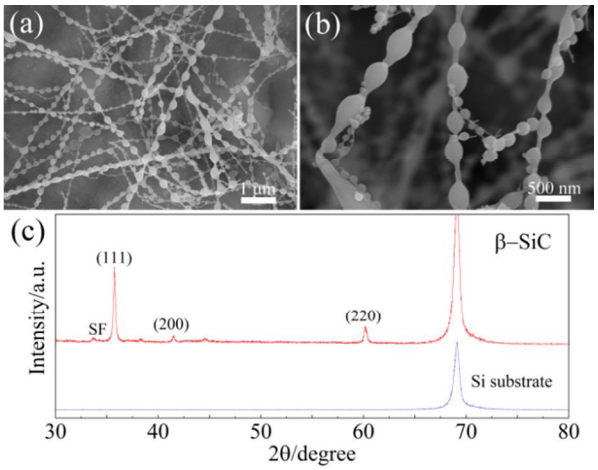

Fig. 1 (a) Low-magnification and (b) high-magnification FESEM images of the chainlike nanostructures prepared from a simplified thermal evaporation method; (c) X-ray diffraction pattern of the chainlike products.

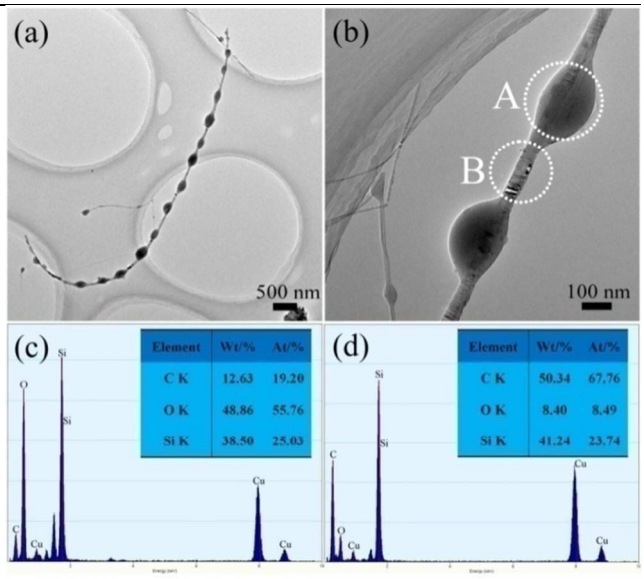

Fig. 2 (a) TEM image of a single nanowire periodically wrapped by nanospheres; (b) Conventional TEM image of the chainlike nanostructures, where the silica layer can be easily distinguished from the SiC core; (c) EDS spectrum of the chainlike nanostructures recorded from the marked area A in (b); (d) EDS spectrum taken from the marked area B in (b).

Results and discussion

Figs. 1a-b show the FESEM images of as-fabricated products directly grown on a rectangle silicon wafer via a simplified thermal evaporation method without using catalyst, template and flowing gases (Ar, CH_4, N_2, *etc.*). Lots of chainlike nanostructures homogeneously distribute on the silicon wafer (Fig. 1a). The amount of the chainlike nanostructures in the sample exceeds 80%, which indicates the relatively high amount and purity quotient of the products. The length of the nanochains ranges from several to tens of microns (Fig. 1a), and the bead size of the nanochains is not of uniform size, which are ranged from 100 nm to 300 nm (Fig. 1b). Fig. 1c shows the X-ray diffraction (XRD) pattern of the products. As Fig. 1c indicated, in addition to the peak from the Si substrate, the other peaks match well with the standard diffraction pattern of β-SiC phase (JCPDS card no. 29-1129). The strong intensities and narrow widths of the peaks indicated that the chainlike nanostructures were crystalline. A small peak ahead of the highest intensity peak (111) is assumed due to stacking faults.

Fig. 2 depicts the TEM observation taken on a single chainlike nanostructure and the EDS spectrum of the chainlike nanostructure record from the marked area A and B. As is obviously shown in Fig. 2a, a single nanowire periodically wrapped by nanospheres has been prepared. What's more, no catalyst tips are found at the tip of the nanochain. Fig. 2b reveals that the thick layer can be easily distinguished from the core. Figs. 2c and d are the EDS spectrum of the chainlike nanostructure

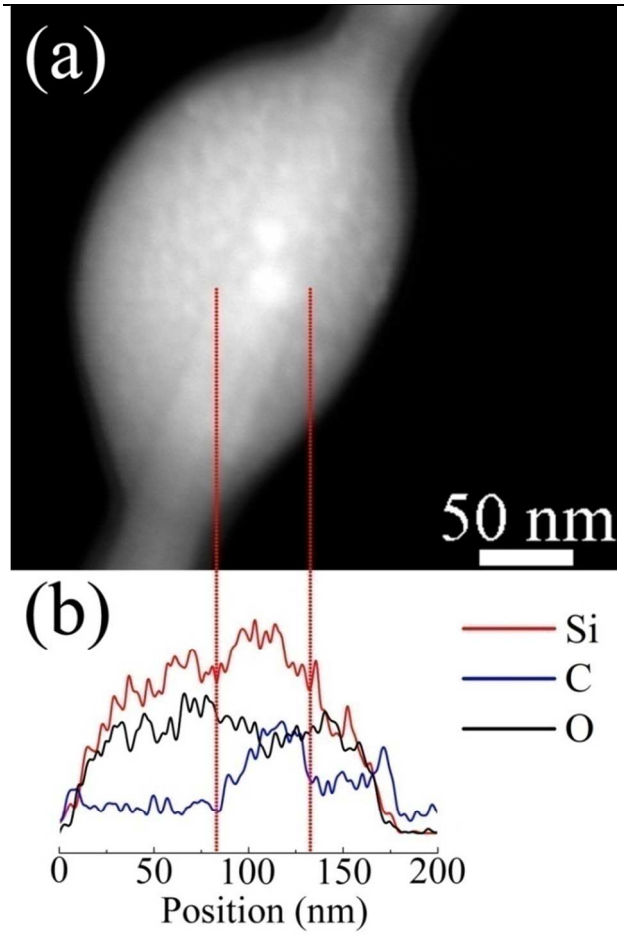

Fig. 3 (a) A typical STEM image of the nanochains, where the thick layer can be easily distinguished from the core; (b) Cross-sectional elemental line-scanning showing the Si (red line), C (blue line) and O (dark line) concentrations. The solid lines show the theoretical cross-section for a 50 nm diameter core.

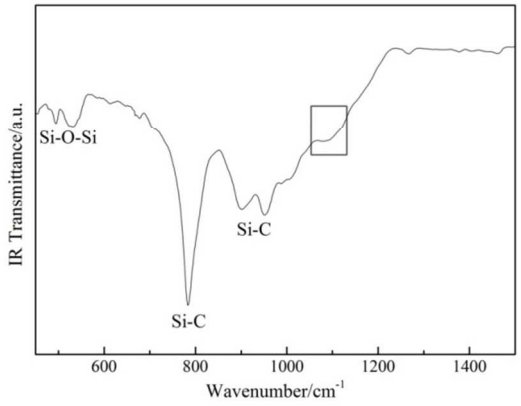

Fig. 4 FT-IR absorbance spectrum of SiC/SiO_x nanochain heterojunctions.

recorded from the nanosphere (the marked area A in Fig. 2b) and the nanowire between nanospheres (the marked area B in Fig. 2b). The EDS analysis reveals that both the nanowire and the nanosphere are composed of Si, C and O whereas the O content in the bead is extremely higher than it in the nanowire. The corresponding detailed data are shown inset in Figs. 2c and d. On account of the results, we roughly consider the nanochains are composed of SiC-core nanowires and SiO_x wrapping shell.

In order to characterize the elemental content in detail, STEM analysis with cross-sectional elemental line-scanning is also conducted. From the STEM image (Fig. 3a), we confirm that the chainlike nanostructure possess a core-shell structure. Fig. 3b is the analysis of cross-sectional elemental mapping data, which also reveal a core-shell structure that is consistent with SiC-core and SiO_x-shell. Fig. 3b shows that the SiC core is about 50 nm.

In addition, FT-IR is also used to confirm the composition of the nanochains. As shown in Fig. 4, the absorption peak at around 784 cm^{-1} corresponds to the transversal optic (TO) Si-C stretching vibration and the peaks at around 890-950 cm^{-1} is related to the longitudinal optic (LO) vibration mode. Moreover, there are two absorption peaks at around 493 cm^{-1} and 529 cm^{-1}, which corresponds to Si-O-Si stretching vibration of amorphous SiO_x. [6] The shoulder at around 1064-1100 cm^{-1} is matched with Si-O stretching vibration. Together with the FESEM, TEM, STEM, EDS analyses, we believe that the as-prepared nanochains consists mainly of SiC-core wrapped with amphorous SiO_x nanospheres.

HRTEM and SAED analyses are conducted to further investigate the structures in detail. Fig. 5a displays the typical TEM image as exhibited in Fig. 2b. As we can see, the SiC core goes through the nanospheres along its length and has a consistent diameter (about 50 nm). The thickness of the SiO_x shell at the sphere areas is about 40-120 nm. Fig. 5b displays a HRTEM image of the nanowire marked by a dashed rectangle in Fig. 5a, which shows that the nanowire is structurally uniform without obvious defects and suggests the outer layers of the SiC-core are amorphous. The *d*-spacing between two adjacent lattice fringes is 0.25 nm for the string, corresponds to the (111) plane of 3C-SiC and suggests that the SiC/SiO_x nanochain heterojunctions grow along [111] direction. Moreover, Fig. 5b also illustrates the typical thickness of the SiO_x shell is about 3 nm at the nanowire areas. Fig. 5c is also a HRTEM image of a nanowire between nanospheres. From the HRTEM image, one can see a biaxial structure has also been obtained. The inter-planner *d* spacings, 0.25 nm and 0.25 nm in each side, respectively correspond to the (111) planes of 3C-SiC. The corresponding SAED pattern of the biaxial structure is shown in Fig. 5d. The diffraction spots clearly indicate the crystallized structure can also be indexed to crystalline 3C-SiC, demonstrating the existence of biaxial SiC/SiC nanowire. An angle between these two crystal planes can be observed at 166.5°from the HRTEM image and the SAED pattern.

Up to now, literatures reported lots of vapor phase methods to synthesis SiC nanowires, their detailed mechanism might involve the formation of precursors or intermediates as a result of the relatively high temperatures. [23-25] Among all vapor based methods, the vapor-solid (VS), vapor-liquid-solid (VLS), solution-liquid-solid (SLS), oxide-assisted growth mechanism seems to be most popular for generating SiC nanowires. As reported before, [26, 27] the growth of SiC nanowires without metal catalysts has been often demonstrated based on the VS mechanism. VS growth is generally believed to start at nanometric nuclei created in situ and it proceeds along one crystallographic direction.[23-25]

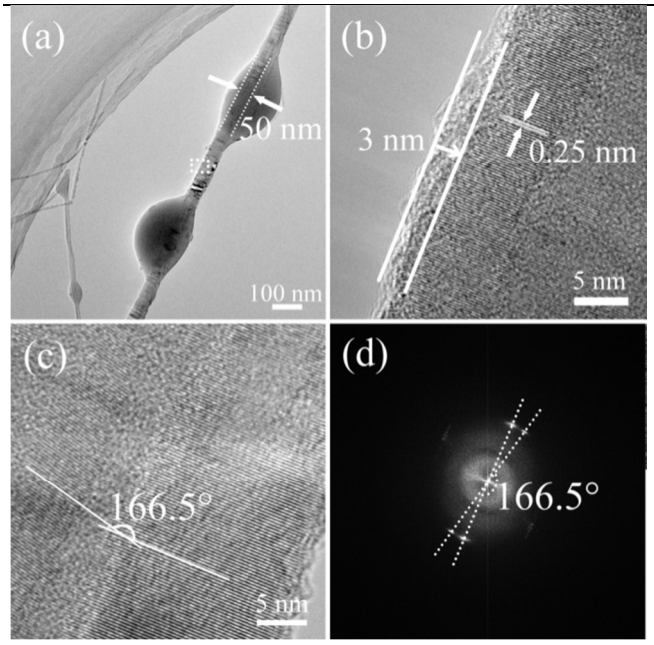

Fig. 5 (a) A typical TEM image of a single SiC/SiO_x nanochain under low magnification; (b) A typical HRTEM image recorded from the marked area A in (a); (c) HRTEM image of the crystalline biaxial SiC nanowire; (d) Corresponding SAED pattern of the biaxial nanowire.

Since the periodic beads are formed in the experiment, simple VS mechanism is inaccurate to demonstrate the formation of SiC/SiO_x nanochains. Bechelany *et al.* [22] synthesized SiC/SiO_2 nanochains by the dewetting of SiO_2 on the surface of SiC, they proposed that the dewetting mechanism has been attributed mainly to the Rayleigh instability. Wei *et al.* [20] and Hou *et al.* [21] all fabricated SiC/SiO_x nanochains by different catalyst-free method. They all proposed that the VS step followed by the modulation process attributed to the form of the SiC/SiO_x nanochains.

In this work, no metallic catalyst was introduced and no metallic droplets were observed at the tips of the nanochains. It suggests that the growth of SiC-core nanowire is attributed to the VS mechanism. Based on the previous researches and the experimental results, VS process followed by a modulation step is proposed to demonstrate the formation of the nanochains. Figs. 6a-b shows a schematic illustration for the growth of SiC/SiO_x nanochain heterojunctions.

Previously, some literatures reported the synthesis of SiC nanowires via chemical vapor deposition method. For example, Chen *et al.* [26] fabricated a large scale number of SiC nanowires by a simiple catalyst-free method using silicon powders and expandable graphite as raw materials. Chen *et al.* [28] synthesized SiC nanowires on Si substrate by the thermal evaporation method without the assistance of a metal catalyst. The VS mechanism reported by these previous researches was proposed to explain the growth of SiC-core nanowires. The proposed growth procedure was illustrated in Fig. 6a. Before temperature was heated up, there were still unexpelled gases in the reaction system. The intensity of pressure in this system is the atmospheric pressure (1.0×10^5 Pa). The partial pressure of oxygen is about 2.1×10^4 Pa which is even stronger than that of reported before. When the temperature rise gradually, the oxygen react with the graphite powder to CO, and then, the graphite is vapourized to form C vapor. Afterwards, SiO vapor is produced on account of the SiO_x layer on the Si wafer reacts with C vapor, CO vapor, and Si substrate. As previously reported, [27] SiO vapor reacted further with CO according to reactions (1) and (2). Based on the aforementioned reactions, SiC nuclei are generated on the Si substrate, as shown in Fig. 6a. On account of the lowest-energy principle, the SiC-core nanowires always grew along the [111] direction.[29] Fig. 6a shows the proposed mechanism underpinning such a VS process.

$$SiO_{(g)} + 3CO_{(g)} \rightarrow SiC_{(s)} + 2CO_{2(s)} \quad (1)$$

$$Si_{(s)} + 2CO_{(g)} \rightarrow SiC_{(s)} + CO_{2(s)} \quad (2)$$

However, it produces a type of chain-like nanostructure in this research rather than conventional monocrystal nanowires. We propose a modulation procedure lead to the formation of the nanochains as shown in Fig. 6b. As a result of no flowing gas is used in this research, therefore, the content of oxygen was limited. Previous researches indicated that part of SiO vapor phase could react with C (g) and CO (g) (reactions (3-4)), lead to the formation of viscous SiO_x on the surface of the as-grown SiC-core nanowires. [21, 28] It is worth noting that the excess SiO has an important role in determining the diameters of SiO_x beads. Hou *et al.* [21] studied the effect of SiO vapor in the formation of SiO_2 beads by means of adjusting the contents of polyaluminasilazane

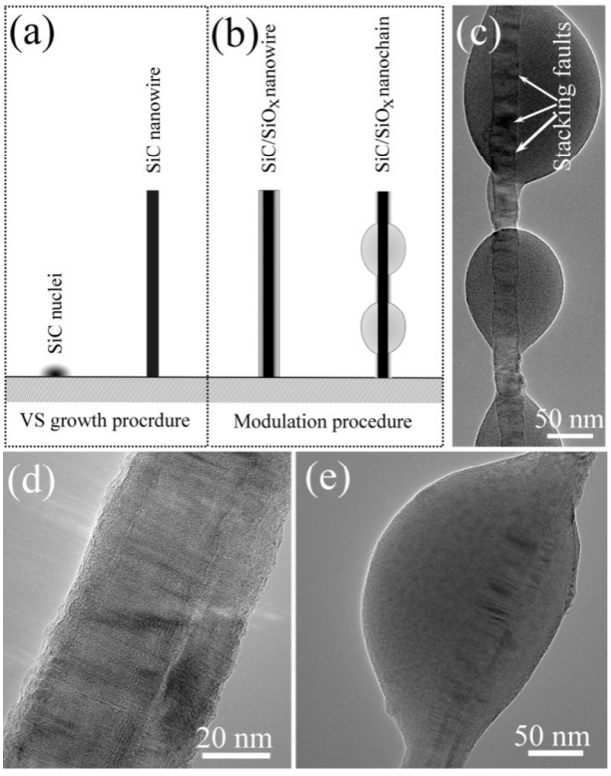

Fig. 6 (a)-(b) Schematic illustration for the growth of SiC/SiO_x nanochains; (c)-(e) Typical TEM images of a single nanochain, in which the SiC nanowire has a high stacking fault inside the SiO_x beads.

(PSN). The generated liquid SiO_x flows along the SiC-core nanowires and covers their surfaces as shown in Fig. 6b. Both Wei *et al.* [20] and Hou *et al.* [21] revealed that the Rayleigh instability and the poor wettability between SiC and SiO_x lead to the liquid SiO_x broken apart and assembled into spherical nanodroplets.

$$3SiO_{(g)} + CO_{(g)} \rightarrow SiC_{(s)} + 2SiO_{2(s)} \quad (3)$$

$$2SiO_{(g)} + C_{(g)} \rightarrow SiC_{(s)} + SiO_{2(s)} \quad (4)$$

Moreover, in this research, we observe that the stacking faults can also affect the formation of SiO_x beads. Fig. 6c is a typical TEM image of a single nanochain, in which we can see that the SiC-core nanowire has high stacking faults inside the SiO_x beads. The SiO_x grow bigger and the SiC-core has more stacking faults. Figs. 6d-e further demonstrates this phenomenon, which is also reported in the previous research.[20] Thus, this is further evidence that the SiO_x beads prefer to grow on the high stacking fault surface of the SiC-core. As reported before, [27, 30, 31] the high stacking faults can lead to a rough surface. The rough surface bring about a higher interface energy. Due to the surface tension of liquid SiO_x, the liquid SiO_x assembles into spherical nanodroplets to minimize its surface energy. [32] The size and eventual morphology of the beads principally depends on the total free energy of the SiO_x droplets and the interfacial energy of SiC/SiO_x and SiO_x/vapor, respectively. [22] Interfacial energy can be denoted by the Young's equation (5), where θ_c is the contact angle, $\sigma_{l\text{-}v}$, $\sigma_{s\text{-}v}$ and $\sigma_{s\text{-}l}$ are the surface tension at the liquid-vapor (*l*-*v*), surface-vapor (*s*-*v*) and solid-liquid (*s*-*l*) interfaces, respectively. When the partial core-bead interfacial energy conforms to this equation, the core-bead area is stable. Therefore, the high stacking faults surface has better wettability.

$$\sigma_{l\text{-}v}\cos\theta_c = \sigma_{s\text{-}v} - \sigma_{s\text{-}l} \quad (5)$$

The photoluminescence spectrum is measured at room temperature for the as-prepared SiC/SiO_x nanochains (Fig. 7). Under excitation at 254 nm from a Xe source, the as-obtained PL line of the SiC/SiO_x nanochains is shown in Fig. 7a (the black line is the emission spectrum, the red and blue line is the simulated line). By using Acq Method, the nanochains show two emission bands at 403 nm (3.08 eV) and 426 nm (2.91 eV) which are both considerably blue-shifted, compared with the band gap of bulk β-SiC at 2.39 eV. The emission line at 426 nm is consistent with the reported data and normally is ascribed the effect of the oxygen discrepancy in the SiO_x shell near the interface boundary and defects related to the oxygen deficiency. [20, 33, 34] Similar emission peaks at about 403 nm were also reported by Meng et al. [5] for the SiC/SiO_2 nanochain heterojunction, which may be ascribed to quantum size effects of the morphology, stress at the SiC/SiO_2 interface boundary and defects. Furthermore, the peak centered at ~400 nm is similar to the previously reported SiC hexagonal nanoprisms or SiC nanobelts. [35, 36] To investigate the difference PL properties between the SiC/SiO_2 nanochains and SiC nanowires, the chainlike product was immersed in HF solution (0.1 M) for 1 h and then its PL property was measured. Fig. 7b shows the PL

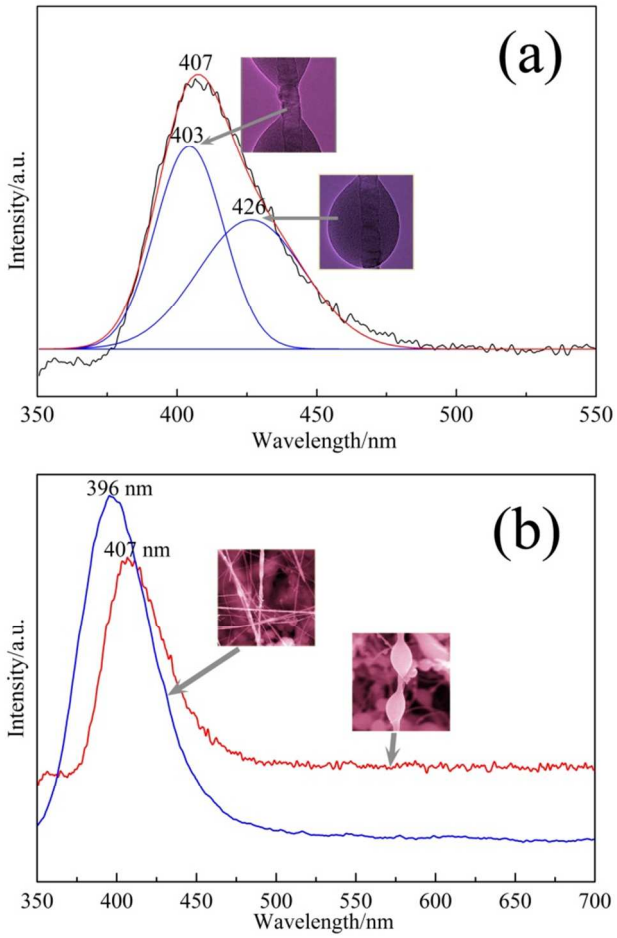

Fig. 7. (a) The emission spectrum of the as-obtained SiC/SiO_x nanochain heterojunctions (the black line is the as-obtained PL line, the red and blue line is the simulated line); (b) the comparison spectra of the SiC nanowires and the nanochains.

spectra of the SiC/SiO_2 nanochains and the SiC nanowires. The nanowires show a symmetrical spectrum at 396 nm (3.13 eV) which is slightly blue- shifted compared with the nanochains. It confirmed that the emission peak at 426 nm is consistent with the SiO_x shell. Moreover, the peak intensity of the nanochains is slightly lower than the nanowires. It suggested the existing of the SiO_x beads may affect the PL intensity of the nanowires. These results suggested that the PL properties of SiC nanowires can be tailored by SiO_x shell or SiO_x beads. On account of the blue-shift emission properties, SiC/SiO_x nanochains prepared via the simplified thermal chemical vapor deposition method may have an application in blue-green emitting diodes and display devices.

Conclusions

In summary, core-shell SiC/SiO_x nanochain heterojunctions have been successfully synthesized on silicon substrate via a simplified thermal evaporation method at 1500 °C without using catalyst, template and flowing gases (Ar, CH_4, N_2, *etc.*). The as-synthesized nanochains were up to tens of microns long and

typically have 40-50 nm diameter single crystalline SiC-core nanowires wrapped by SiO_x nanospheres (40-120 nm in diameter). The SiC-core nanowires were grown along [111] direction with a high density of stacking faults. The growth process was codominated VS growth procedure and modulation procedure. The formation of SiO_x beads not only relates to the Rayleigh instability and the poor wettability between SiC and SiO_x, but also corresponds to the existence of high stacking faults within SiC-core. The intensive blue-green emission properties of the SiC/SiO_x nanochains are of significant interest for their potential blue-green emitting devices. Our study presented here will be helpful in simplify designing and preparing other Si-C related heterostructures, simultaneously, this preparing method could be applied to prepare a large number of SiC nanostructures.

Acknowledgements

This work was supported by the National Natural Science Foundation of China (Grant No. 51032007) and the Research Fund for the Doctoral Program of Higher Education of China (Grant No. 20130022110006). Xiaowen Wu also thanks the Beijing Higher Education Young Elite Teacher Project (Grant No.YETP0636) and the National Natural Science Foundation of China (Grant No.51372232).

Notes and references

[a]*School of Materials Science and Technology, China University of Geosciences(Beijing), Beijing 100083, P.R.China. Fax: +861082322186; Tel: +861082322186; E-mail: huang118@cugb.edu.cn.*

[b]*College of Engineering, Mathematics and Physical Sciences, University of Exeter, Exeter EX4 4QF, UK.*

1 S.Iijima,*Nature*, 1991, **354**, 56-58.
2 R. B. Wu, G. Y. Yang, M. X. Gao, B. S. Li, J. J. Chen, R. Zhai and Y. Pan,*Cryst. Growth Des.*, 2008, **9**, 100-104.
3 J. T. Huang, Z. H. Huang, Y. G. Liu, M. H. Fang, K. Chen, Y. T. Huang, S. F. Huang, H. P. Ji, J. Z. Yang, X. W. Wu and S. W. Zhang, *Nanoscale*, 2014, **6**, 424-432.
4 W. Xie, G. Möbus and S. W. Zhang,*J. Mater. Chem.*, 2011, **21**, 18325-18330.
5 A. L. Meng, M. Zhang, W. D. Gao, S. B. Sun and Z. J. Li,.*Nanoscale Res. Lett.* 2011, **6**, 34.
6 Z. J. Li, W. D. Gao, A. L. Meng, Z. D. Geng, and L. Gao, *J. Phys. Chem. C,* 2008, **113**, 91-96.
7 A.J. Mieszawska, R. Jalilian, G.U. Sumanasekera and F.P. Zamborini, *Small*, 2007, **3**, 722-756.
8 H. Cui, L. Gong, Y. Sun, G. Z. Yang, C. L. Liang, J. Chen, and C. X. Wang, *CrystEngComm,* 2011, **13**, 1416-1421.
9 K. Chen, M. H. Fang, Z. H. Huang, J. T. Huang and Y. G. Liu, *CrystEngComm*, 2013, **15**, 9032-9038.
10 L.J. Lauhon, M.S. Gudiksen, D. Wang and C.M. Lieber, *Nature*, 2002, **420**, 57-61.
11 D. Moore, J.R. Morber, R.L. Snyder and Z.L. Wang, *J. Phys. Chem. C*, 2008, **112**, 2895-2903.
12 M. Rafiq, Z. Durrani, H. Mizuta, A. Colli, P. Servati, A. Ferrari, W. Milne and S. Oda, *J. Appl. Phys.*, 2008, **103**, 053705-053704.
13 Y. Tak, Y. Ryu and K. Yong, *Nanotechnology*, 2005, **16**, 1712.
14 Y. Li, P.S. Dorozhkin, Y. Bando and D. Golberg, *Adv. Mater.*, 2005, **17**, 545-549.
15 K. Saulig-Wenger, M. Bechelany, D. Cornu, T. Epicier, F. Chassagneux, G. Ferro, Y. Monteil and P. Miele, *J. Phys. IV*, 2005,**124**, 99-102.
16 Y. Li, Y. Bando and D. Golberg, *Adv. Mater.*, 2004, **16**, 93-96.
17 H.Y. Kim, S.Y. Bae, N.S. Kim and J. Park, *Chem. Commun.*, 2003, **20**, 2634-2635.
18 Y.Q. Zhu, W.B. Hu, W.K. Hsu, M. Terrones, N. Grobert, T. Karali, H. Terrones, J.P. Hare, P.D. Townsend and H.W. Kroto, *Adv. Mater.*, 1999, **11**, 844-847.
19 M. O'Brien, C. Koitzsch and R. Nemanich, *J. Vac. Sci. Techno. B*, 2000, **18**, 1776-1784.
20 G. D. Wei, W. P. Qin, K. Z. Zheng, D. S. Zhang, J. B. Sun, J. J. Lin, R. Kim, G. F. Wang, P. F. Zhu and L. L. Wang, *Cryst. Growth Des.,* 2009, **9**, 1431-1435.
21 H. L. Hou, L. Wang, F. M. Gao, G. D. Wei, J. J. Zheng, X. M. Cheng, B. Tang and W. Y. Yang, *CrystEngComm,* 2013, 15, 2986-2991.
22 M. Bechelany, J.L. Riesterer, A. Brioude, D. Cornu and P. Miele, *CrystEngComm*, 2012, **14**, 7744-7748.
23 Y. N. Xia, P. D. Yang, Y. G. Sun, Y. Y. Wu, B. Mayers,B. Gates, Y. D. Yin, F. Kim and H. Q. Yan,*Adv. Mater.*,2003,**15**, 353–389.
24 K. Zekentes and K. Rogdakis, *J. Phys. D: Appl. Phys.*, 2011, **44**, 133001.
25 Y. D. Yin, F. Kim and H. Q. Yan, *Adv. Mater.*, 2003, **15**, 353-389.
26 J. J. Chen, Q. Shi, L. P. Xin, Y. Liu, R. J. Liu and X. Y. Zhu, *J. Alloy. Compd.,* 2011, **509**, 6844-6847.
27 Z. H. Huang, H. T. Liu, K. Chen, M. H. Fang, J. T. Huang, S. Y. Liu, S. F. Huang, Y. G. Liu, and X. W. Wu, *RSC Adv.,* 2014, **4**, 18360-18364.
28 K. Chen, Z. H. Huang, J. T. Huang, M. H. Fang, Y. G. Liu, H. P. Ji and L. Yin, *Ceram. Int.,* 2013, **39**, 1957-1962.
29 L. Wang, H. Wada and L. F. Allard, *J. Mater. Res*., 1992, **7**, 148.
30 D. H. Wang, D. Xu, Q. Wang, Y. J. Hao, G. Q. Jin, X. Y. Guo and K. N. Tu, *Nanotechnology*, 2008, **1**9, 215602.
31 Y. T. Zhai and X. G. Gong, *Phys. Lett. A,* 2011, **375**, 1889-1892.
32 M. Bechelany, X. Maeder, J. Riesterer, J. Hankache, D. Lerose, S. Christiansen, J. Michler and L. Philippe, *Cryst. Growth Des.*, 2010, **10**, 587-596.
33 R. B.Wu, B. L.Zha, L. Y.Wang, K.Zhou and Y.Pan, *Phys. Status Solidi (a)*., 2012, **209**, 553-558.
34 Y. P.Guo, J. C.Zheng, A. T. S.Wee, C. H. A.Huan, K.Li, J. S.Pan, Z. C.Feng and S. J.Chua, *Chem. Phys. Let.* 2001, **339**, 319-322.
35 R. B. Wu, G. Y. Yang, Y. Pan and J. J. Chen, *Appl. Phys. A,* 2007, **86**, 271-274.
36 G. C. Xi, Y. Y. Peng, S. M. Wan, T. W. Li, W. Chao and Y. T. Qian, *J. Phys. Chem. B,* 2004, **108**, 20102.

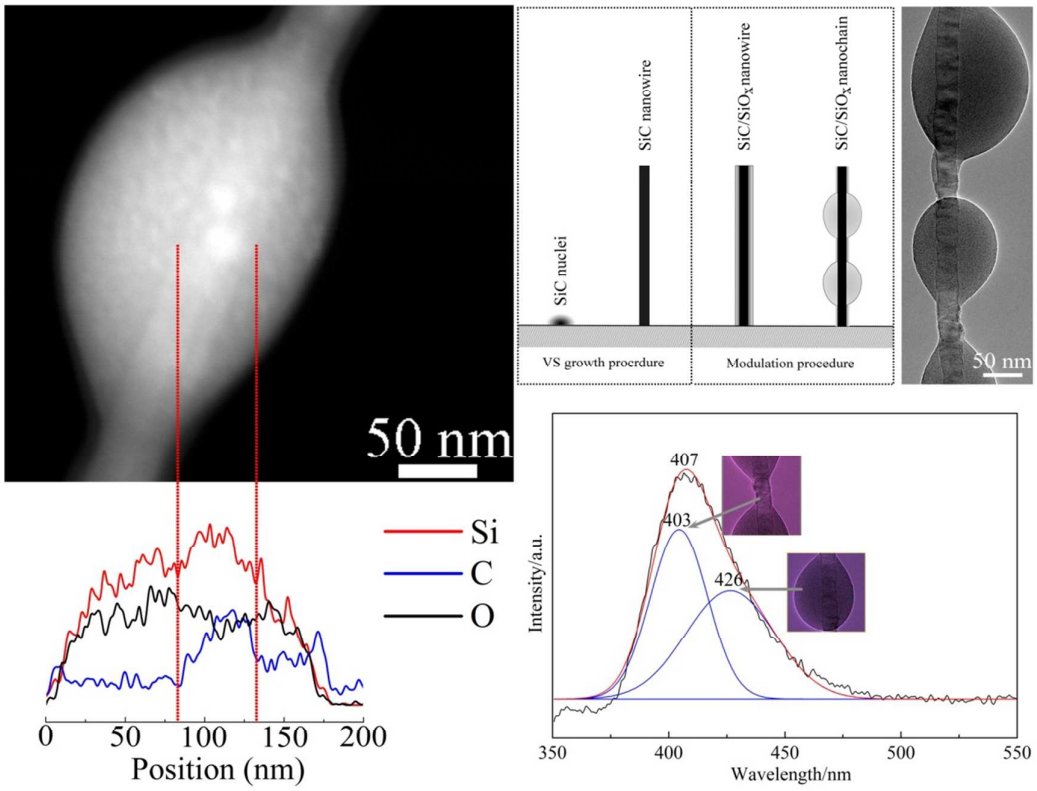

Highlight:

Chainlike SiC/SiO_x heterojunctions were prepared on a silicon wafer by a simplified catalyst-free thermal chemical vapour deposition (CVD) method.